

# Study of the Kitaev Models

*Project report submitted by*

**Arnab Barman Ray**

3rd Year Int. Msc

Indian Institute Of Technology Kharagpur

May 2016 - July 2016

Supervisor: Dr.Saurabh Basu

Department of Physics

Indian Institute of Technology Guwahati 781 039, India

July, 2016

# Abstract

In this project we numerically reproduce some of the results obtained by Kitaev in two of his models- the Kitaev Chain and the Kitaev honeycomb lattice. We see how the Kitaev Chain exhibits unpaired Majorana Modes which gives rise to robust degenerate ground states in a certain part of the parameter space. These ground states are such that both phase error and classical error can be avoided thus helping in fault-tolerant quantum computation. We also numerically investigate the bulk spectrum and see how a phase transition takes place as we move from one part of the parameter space to another. We generate the Density of states for the Kitaev Honeycomb matrix for 450 lattice sites. We also see how phase transitions take place when we change the spin-coupling parameters.

# Contents

<b>1</b>	<b>The Kitaev Chain</b>	<b>5</b>
1.1	The Hamiltonian And Majorana Operators . . . . .	5
1.2	Two special cases . . . . .	7
1.3	General conditions for Majorana Operators . . . . .	8
1.4	The Bulk Spectrum . . . . .	11
<b>2</b>	<b>The Kitaev Honeycomb</b>	<b>14</b>
2.1	Lattice and the Hamiltonian . . . . .	14
2.2	Jordan-Wigner Transformation and related Operators . . . . .	15
2.3	The Bulk Spectrum . . . . .	16

# List of Figures

1.1	Coupling between the Majorana Modes[7]	6
1.2	DOS for the trivial(up) and topological(down) case	7
1.3	Energy difference between the two ground states,(left)linear scale,(right)logarithmic scale for $\mu = 10, w = 7$ and $ \Delta  = 3$	10
1.4	Trivial DOS 1 & 2	11
1.5	Critical Point	11
1.6	Topological DOS 1 & 2	12
1.7	Spectra at different parameter values	13
2.1	The Honeycomb lattice.[9]	14
2.2	Plaquette Operator	15
2.3	Unit Cell[8]	16
2.4	The Phase Diagram	17
2.5	Gapless phase	18
2.6	Borderline gapped phase	18
2.7	Gapped Phase	18
2.8	Phase transitions	19
2.9	DOS for different coupling parameters	19

# Chapter 1

## The Kitaev Chain

### 1.1 The Hamiltonian And Majorana Operators

In his paper[1], Kitaev introduced a toy model which simulates the properties of a wire placed on the surface of a p-wave superconductor. The wire has  $L$  fermionic sites which can be occupied or unoccupied by spinless fermions. The  $j$ th state is given by the wavefunction  $\delta(x-j)$ . In basis of these states, Kitaev introduces the Hamiltonian, in the language of second quantization[5] as:

$$H = \sum_j (-w(a_j^\dagger a_{j+1} + a_{j+1}^\dagger a_j) - \mu(a_j^\dagger a_j - \frac{1}{2}) + \Delta a_j a_{j+1} + \Delta^* a_{j+1}^\dagger a_j^\dagger) \quad (1.1)$$

Here,  $a_j$  and  $a_j^\dagger$  follow the usual fermionic anti-commutation relations,

$$\{a_j, a_k\} = 0 \quad \{a_j^\dagger, a_k^\dagger\} = 0 \quad \{a_j, a_k^\dagger\} = \delta_{jk} \quad (1.2)$$

$w$  is the hopping amplitude,  $\mu$  is the chemical potential and  $\Delta$  is the superconducting gap. We absorb the phase of the superconducting gap while defining the Majorana Operators:

$$c_{2j-1} = e^{i\theta/2} a_j + e^{-i\theta/2} a_j^\dagger \quad c_{2j} = -ie^{i\theta/2} a_j + ie^{-i\theta/2} a_j^\dagger \quad (1.3)$$

where  $\theta$  is obtained from the superconducting gap,  $\Delta = |\Delta|e^{i\theta}$

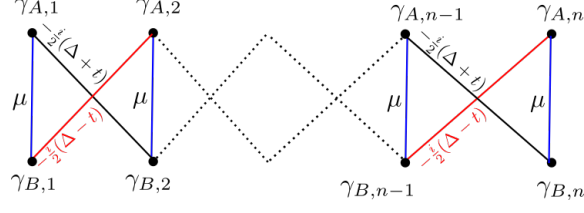


Figure 1.1: Coupling between the Majorana Modes[7]

In terms of these Majorana Operators, the hamiltonian can be rewritten as:

$$H = i/2 \sum_j [-\mu c_{2j-1} c_{2j} + (w + |\Delta|) c_{2j} c_{2j+1} + (-w + |\Delta|) c_{2j-1} c_{2j+2}] \quad (1.4)$$

As we can clearly see from (1.2), the transformation is orthogonal and each fermionic site gives rise to two Majorana Modes which are hermitian, i.e  $c_k^\dagger = c_k$ . The orthogonal transformation ensures the following properties for the modes:

$$\{c_j, c_k\} = 2\delta_{jk} \text{ and } c_j^2 = 1$$

It is instructive to think of an electron to be made up of two Majorana quasi-particles but one has to be careful because the Majorana modes themselves do not represent particles which could physically exist because the number operator constructed as:  $c_j^\dagger c_j = c_j^2 = 1$  and hence makes no sense.

It is more correct to think in terms of combinations of majorana modes which gives rise to fermionic excitations such as in (1.2),  $a_j^\dagger = \frac{1}{2} e^{i\theta/2} (c_{2j-1} - i c_{2j})$ .

The fermionic number operator,  $a_j^\dagger a_j = \frac{(1 + i c_{2j-1} c_{2j})}{2}$ . Hence,  $(i c_{2j-1} c_{2j}) = 1$  or  $-1$  depending on whether the fermionic site is occupied or unoccupied.

We define the Parity operator as:  $P = \prod_j (-i c_{2j-1} c_{2j})$ .  $P$  commutes with the Hamiltonian  $\mathbf{H}$  in (1.3). The eigenstates of  $\mathbf{H}$  hence have definite parity i.e  $P = -1$  or  $+1$ , depending on whether they have an odd or even number of fermions.

A real orthogonal transformation of the Majorana operators given as  $\vec{c}' = M \vec{c}$  where  $M M^T = 1$ , might or might not change the fermionic parity  $P = (-i)^L \prod_j c_j = \det(M) (-i)^L \prod_j c'_j$  of a state.

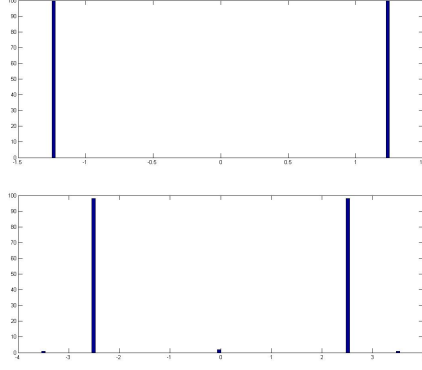


Figure 1.2: DOS for the trivial(up) and topological(down) case

## 1.2 Two special cases

Now we look at two special cases of the Hamiltonian:

(a) The trivial case:  $\Delta = w = 0$  and  $\mu < 0$  we get the hamiltonian:

$$H_a = -\mu \sum_j (a_j^\dagger a_j - \frac{1}{2}) = \frac{i}{2}(-\mu) \sum_j c_{2j-1} c_{2j} \quad (1.5)$$

So, the Majorana operators from a single site are paired together to give rise to the original electrons. The ground state has occupation number 0.

(b) The topological case:  $\Delta = w > 0$  and  $\mu = 0$ .

$$H_b = iw \sum_j c_{sj} c_{2j+1} = 2w \sum_{j=1}^{L-1} (\tilde{a}_j^\dagger \tilde{a}_j - \frac{1}{2}) \quad (1.6)$$

As we can see the Majorana modes from neighbouring sites are coupled. The operators  $c_1$  and  $c_{2L}$  do not appear in the Hamiltonian. New fermionic modes constructed as  $\tilde{a}_j = \frac{1}{2}(c_{2j} + ic_{2j+1})$  are the eigenmodes of this phase.

Now, we can construct a non-local fermionic mode from the two Majorana operators that are left out from the hamiltonian,  $f^\dagger = \frac{1}{2}(c_1 - ic_{2L})$  is a  $-w$  energy fermionic eigen-mode of the Hamiltonian. The ground state of (1.5) must satisfy  $\tilde{a}_j |\Phi_0\rangle = 0 \quad \forall \quad j$ . Hence the parity operator  $P$  reduces to the form,  $-ic_1 c_{2L}$ . Now, both  $c_1$  and  $c_{2L}$  commutes with  $H_b$ . (this implies that the ground state of the Hamiltonian is an eigenstate of both the Majorana operators). So does  $P$ . If  $|\Phi_0\rangle$  is the ground state, it can be shown that

both  $c_1|\Phi_0\rangle$  and  $c_{2L}|\Phi_0\rangle$  cannot be equal to  $|\Phi_0\rangle$ . Hence, a degeneracy in the ground state exists. Infact the two ground states  $|\Phi_0\rangle$  and  $|\Phi_1\rangle$  represent non-occupation and occupation of the non-local fermionic mode  $f^\dagger$ .

$$|\Phi_0\rangle = |0\rangle_f \Pi_{j=1}^{l-1} |0\rangle_j \text{ and } |\Phi_1\rangle = |1\rangle_f \Pi_{j=1}^{l-1} |0\rangle_j \quad (1.7)$$

The two modes can be swapped between each other by an operation of  $c_1, c_{2L}$  or  $f^\dagger$ . Also,  $P|\Phi_0\rangle = +1$  and  $P|\Phi_1\rangle = -1$ , representing odd and even fermionic states. Since they involve a non-local mode, local perturbations cannot lift the degeneracy as they cannot contain both of the two majorana modes. Hence these states can be used in non-local storage of information.

### 1.3 General conditions for Majorana Operators

The Hamiltonian in (1.3) can be written in a matrix form in the Majorana matrix,

$$H = \frac{i}{4} C^\dagger \mathbf{H} C \text{ where } C = [c_1, c_2, \dots, c_{2L}] \quad (1.8)$$

where the matrix  $\mathbf{H}$  has the form:

$$\mathbf{H} = \begin{pmatrix} 0 & -\mu & 0 & (-w + |\Delta|) & 0 & 0 \dots \\ \mu & 0 & (w + |\Delta|) & 0 & 0 & 0 \dots \\ 0 & -(w + |\Delta|) & 0 & -\mu & 0 & (-w + |\Delta|) \dots \\ (w - |\Delta|) & 0 & \mu & 0 & (w + |\Delta|) & 0 \dots \\ \vdots & \vdots & \vdots & \vdots & \vdots & \ddots \end{pmatrix}$$

$\mathbf{H}$  is a skew-symmetric matrix. This means that it has purely imaginary eigenvalues of the form:  $\pm i\epsilon_m$ . We try to find solutions for one of the eigenvalues to be zero.

$\mathbf{H}$  can be reduced to the block-diagonal form by a real orthogonal matrix  $W$  like:

$$A = W \mathbf{H} W^T = \begin{pmatrix} 0 & \epsilon_1 & 0 & 0 \dots \\ -\epsilon_1 & 0 & 0 & 0 \dots \\ 0 & 0 & 0 & \epsilon_2 \dots \\ 0 & 0 & -\epsilon_2 & 0 \dots \\ \vdots & \vdots & \vdots & \vdots & \vdots & \ddots \end{pmatrix} \quad (1.9)$$

So, now the Hamiltonian is of the form  $H = \sum_m \epsilon_m b'_m b_m$ .



We try to find the conditions on  $W$  so that one of the eigenvalues is zero, Any skew-symmetric matrix  $\mathbf{H}$  can be block-diagonalized by utilizing it's eigenvectors.

$\mathbf{H}\vec{u}_m = +i\epsilon_m \implies \mathbf{H}\vec{u}^* = -i\epsilon_m$  We define new real vectors  $\xi_m = i(u_m^* - u_m)/2$  and  $\eta_m = (u_m + u_m^*)/2 \implies \mathbf{H}\xi_m = -\epsilon_m\eta_m$  and  $\mathbf{H}\eta_m = \epsilon_m\xi_m$ .

The transformation matrix  $W$  is defined as[6]:

$$W_{2j-1} = [\eta_j^T] \text{ and } W_{2j} = [-\xi_j^T] \quad (1.10)$$

It can be shown that  $W$  is orthogonal. In his paper, Kitaev employs an ansatz of the form:

$$b' = \sum_j (\alpha'_+ x_+^j + \alpha'_- x_-^j) c_{2j-1}, \quad b'' = \sum_j (\alpha''_+ x_+^{-j} + \alpha''_- x_-^{-j}) c_{2j-1} \quad (1.11)$$

Using the form of  $W$ , it can be shown in the limit  $L \rightarrow \infty$ , that the conditions are perfectly satisfied with  $\epsilon_m = 0$  if  $x_{\pm} = \frac{-\mu \pm \sqrt{\mu^2 - 4w^2 + 4|\Delta|^2}}{2(w + |\Delta|)}$ , in the parameter space  $2w > \mu$ ,  $|\Delta| \neq 0$ .

For finite  $L$  however, the two ground states are separated by an energy difference of  $2\epsilon \propto e^{-L/l_0}$ .

This has been verified for chains upto 80 sites long in Figure 1.3. The linear fitting gives the power of the exponential to be proportional to  $-0.4568$ , which is not very close to the theoretical value of  $-0.5039$  (an error of 9.35 %). This may be attributed to numerical inaccuracy for large matrices.

We verify the division of parameter space of the Hamiltonian into two parts one of which exhibits Majorana Zero Modes i.e when  $2w > |\mu|$ . When  $|2w| < |\mu|$ , the Hamiltonian does not contain unpaired Majorana fermions and zero modes are non-existent.

We start with the values  $\mu = 10$ ,  $w = 4$  and  $|\Delta| = 3$  and serially increase the value of  $w$  by 0.5 and plot the resulting five histograms which depict the density of states.

As expected, there are no Majorana Zero Modes when  $\mu = 10$ ,  $w = 4$  (left) and  $|\Delta| = 3$  (right). A similar case is exhibited by  $\mu = 10$ ,  $w = 4.5$  and  $|\Delta| = 3$ . Both the cases are gapped.

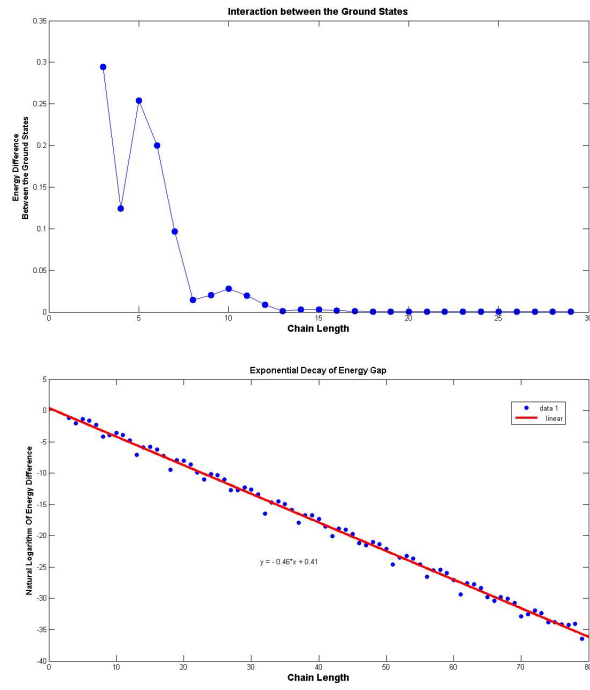


Figure 1.3: Energy difference between the two ground states,(left)linear scale,(right)logarithmic scale for  $\mu = 10, w = 7$  and  $|\Delta| = 3$ —

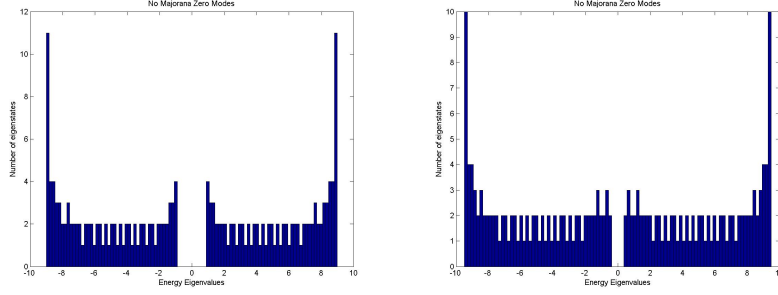


Figure 1.4: Trivial DOS 1 & 2

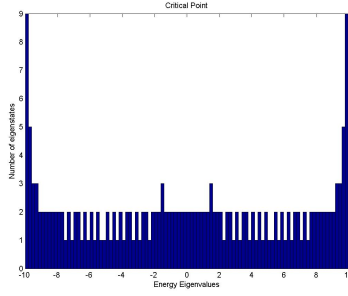


Figure 1.5: Critical Point

At critical point, where  $2w = |\mu| = 10$  does exhibit Majorana zero modes as is found, but the spectrum is gapless and hence the states are not robust.(Figure 1.5)

As expected we can clearly see the zero modes when  $w = 5.5$  and  $\mu = 10$ (left) as well as when  $w = 5.5$  and  $\mu = 10$ (right). Both these spectra are gapped and support robust ground states(Figure 1.6).

## 1.4 The Bulk Spectrum

In this section, we investigate the properties of the bulk spectrum for the chain. We write the original fermionic position operators terms of the creation operators,  $a_k^\dagger$  of the momentum states  $\frac{1}{\sqrt{L}}e^{ikx}$ .

$$a_j^\dagger = \frac{1}{\sqrt{L}} \sum_{k \in FBZ} \langle k | \delta(x - j) \rangle a_k^\dagger \quad (1.12)$$

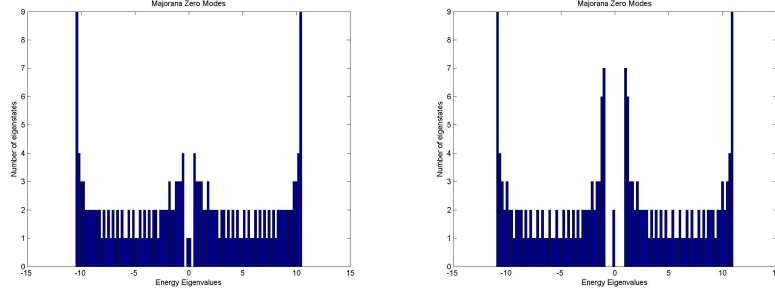


Figure 1.6: Topological DOS 1 & 2

The Hamiltonian(1.1) is then rewritten in the Bogoliubov-deGennes form using contributions from both  $+k$  and  $-k$  operators as:

$$H = \begin{bmatrix} a^\dagger & a_{-k} \end{bmatrix} \begin{bmatrix} -2w \cos k - \mu & -2\Delta^* i \sin k \\ 2\Delta^* i \sin k & 2w \cos k + \mu \end{bmatrix} \begin{bmatrix} a_k \\ a_{-k}^\dagger \end{bmatrix} \quad (1.13)$$

Diagonalizing this we end up with the spectrum:

$$\epsilon(k) = \pm \sqrt{(2w \cos k + \mu)^2 + 4|\Delta|^2 \sin^2 k} \quad (1.14)$$

The diagonalized Hamiltonian is:  $H = \sum_k \epsilon_k \tilde{a}_k^\dagger \tilde{a}_k + \text{constant}$ , where the operators  $\tilde{a}_k^\dagger = u_k a_k + v_k a_{-k}^\dagger$  and

$$u_k = \frac{\Delta_k}{|\Delta_k|} \left( \frac{\epsilon_k + (2w \cos k + \mu)}{2\epsilon_k} \right)^{1/2} \text{ and } v_k = \left( \frac{\epsilon_k - (2w \cos k + \mu)}{\Delta_k^*} \right) u_k \quad (1.15)$$

, where  $\Delta_k = -2\Delta^* i \sin k$ .

The spectrum is shown below for different values of the parameters. we see the phase is gapless at the critical point:  $\mu = 2w$ .

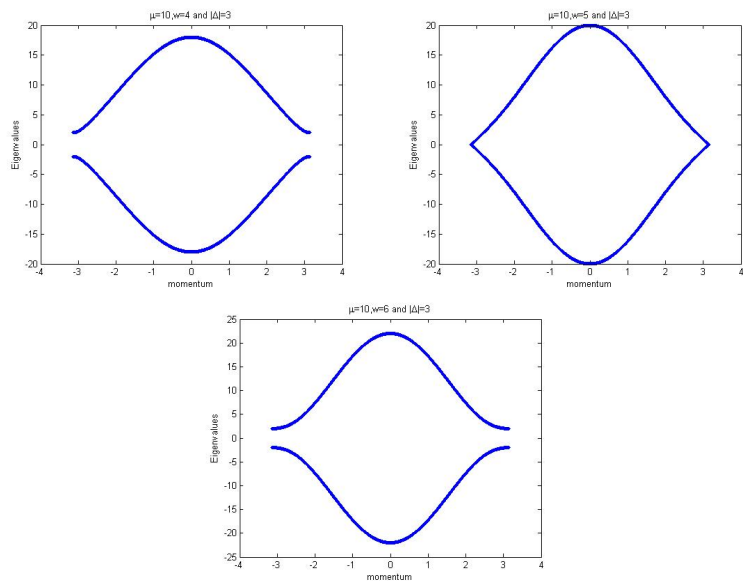


Figure 1.7: Spectra at different parameter values

# Chapter 2

## The Kitaev Honeycomb

### 2.1 Lattice and the Hamiltonian

In his paper[2] Kitaev introduced the Honeycomb lattice as two triangular lattices meshed together:

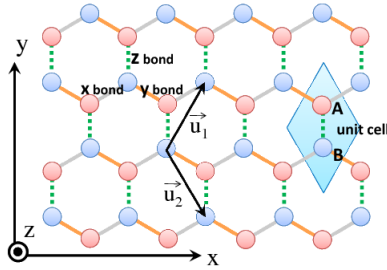


Figure 2.1: The Honeycomb lattice.[9]

The two triangular lattices are respectively termed odd(blue circles) or even(red circles). He also defines three types of links that exist in the model as x-links, y-links and z-links as shown in the picture.

The spin Hamiltonian is of the form:

$$H = -J_x \sum_{x-links} \sigma_j^x \sigma_k^x - J_y \sum_{y-links} \sigma_j^y \sigma_k^y - J_z \sum_{z-links} \sigma_j^z \sigma_k^z \quad (2.1)$$

.  $J_x, J_y$  and  $J_z$  are the coupling parameters.

## 2.2 Jordan-Wigner Transformation and related Operators

Before we proceed to the fermionization of the spin-system, we first look at a conserved quantity called the plaquette operator,  $W_p = \sigma_1^x \sigma_2^y \sigma_3^z \sigma_4^x \sigma_5^y \sigma_6^z$ , where the lattice points are numbered as: Clearly,  $[W_p, H] = 0$ . Hence,  $W_p$  is

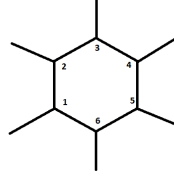


Figure 2.2: Plaquette Operator

a conserved quantity of the eigenstates.

Now, we move on to the fermionization of the system. We introduce new fermionic states for each lattice site  $j$ ,  $a_{1j}^\dagger$  and  $a_{2j}^\dagger$ . The occupation states,  $|1, 1\rangle$  and  $|0, 0\rangle$  represent the up and down spin states of the site respectively. The occupation states,  $|1, 0\rangle$  and  $|0, 1\rangle$  represent unphysical states which we weed out later. Hence, the effect is to extend the space from  $2^N$  dimensions to  $2^{2N}$  dimensions, where  $N$  is the number of lattice points. We define four Majorana operators for each site given be:  $b_x = (a_{1j} + a_{1j}^\dagger)/2$   $b_y = (a_{1j} - a_{1j}^\dagger)/2i$   $b_z = (a_{2j} + a_{2j}^\dagger)/2$   $c = (a_{2j} - a_{2j}^\dagger)/2i$ . They follow the usual ant-commutation rules (1.4).

Since, we have extended the space, we need to project the eigenstates onto the physical space. This is achieved by the operator  $D_j = ib_x b_y b_z c$ . The projection operator is defined as  $D = \prod_j \frac{(1+D_j)}{2}$ . Iff  $D|\Psi\rangle = |\Psi\rangle$ ,  $|\Psi\rangle$  is a physical wavefunction.

To work in the extended space, new Pauli operators are defined as  $\sigma^{alpha} = ib_\alpha c$ . Within the physical space, they have all the properties of the original pauli matrices, as indicated by  $D_j \tilde{\sigma}_j^\alpha = \sigma_j^\alpha$ .

The resulting Hamiltonian is quartic in operators and has the form:

$$H = \frac{i}{4} \sum_{\langle j,k \rangle} A_{jk} c_j c_k \text{ where } A_{jk} = 2J_{\alpha_{jk}} \hat{u}_{jk} \text{ and } \hat{u}_{jk} = ib_j^{\alpha_{jk}} b_k^{\alpha_{jk}} \quad (2.2)$$

Since,  $\hat{u}_{jk}$  (link operator) commute with each other and the Hamiltonian, the Hilbert space can be broken up into direct sums of  $H_u$  where  $u$  is the ordered

set of all values of  $u_{jk}$ . However, since for an assumed physical eigenstate of the link operator,

$$\begin{aligned} \{D_j, \hat{u}_{jk}\} = 0 &\implies D_j \hat{u}_{jk} |\Psi\rangle = -\hat{u}_{jk} D_j |\Psi\rangle \\ \implies D_j \hat{u}_{jk} |\Psi\rangle &= -u_{jk} |\Psi\rangle \implies u_{jk} |\Psi\rangle = -u_{jk} |\Psi\rangle \end{aligned}$$

, the subspaces are not invariant under the projection operator and hence are unphysical. Acting  $D$  on a physical state flips the sign all  $u_{jk}$ . Now, we can use the plaquette operator  $W_p = \prod_{(j,k) \in \text{boundary}(p)} u_{jk}$ . This operator commutes with the hamiltonian and  $D$  which can be seen from the fact the action of  $D$  flips the signs of the  $u_{jk}$  however, since there are six of them in  $W_p$ , it's value remains unchanged. Also, since  $W_p^2 = 1$ , the eigenvalues are  $\pm 1$  for each plaquette.

As it turns out, the lowest energy ground state of the configuration is when

$$W_p = 1 \quad \forall p. \quad (2.3)$$

## 2.3 The Bulk Spectrum

[h] We take a triangular lattice with an associated basis to describe the honeycomb as shown: Using this basis, we write the Hamiltonian as  $H =$

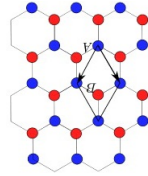


Figure 2.3: Unit Cell[8]

$\frac{i}{4} \sum_{s,\lambda,t,\mu} A_{s\lambda,t\mu} c_{s\lambda} c_{t\mu}$ , where the second indices indicate positions inside the unit cell while the first indicates the lattice site.

We fourier transform the Majorana operators in the case when (2.3) when all  $u_{jk} = 1$ , getting the form:

$$H = \frac{i}{4} \sum_{q,s,t} A_{\lambda,\mu}(q) a_{-q,\lambda} a_{q,\mu}. \quad (2.4)$$



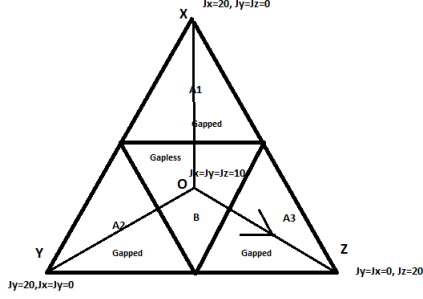


Figure 2.4: The Phase Diagram

Diagonalizing the resulting matrix, we arrive at the spectrum,

$$\epsilon(q) = \pm 2|J_x e^{i(\vec{q} \cdot \vec{n}_1)} + J_y e^{i(\vec{q} \cdot \vec{n}_2)} + J_z|. \quad (2.5)$$

$n_1$  and  $n_2$  are the basis vectors given by:  $(1/2, \sqrt{3}/2)$  and  $(-1/2, \sqrt{3}/2)$ .  $\vec{q}$  is in the reciprocal space of the honeycomb lattice. The three terms of the equation are floating vectors in the 2-D complex space. They can always have a solution if they obey the triangle inequality and vice-versa (due to the triangle law of addition of vectors).

The different phases of the honeycomb can be represented by a slice of the plane  $J_x + J_y + J_z = 1$  in the parameter space. This results in the following triangle: Finding accurately if a spectrum is gapless from the graph of its excitation spectrum is not possible, because even the minimum values (as found from the vectors in matlab) only tend to zero as we decrease the step-size. Hence, say an apparently gapped spectrum with a minimum energy value of 0.05 might in reality be gapless in the exact limit. (Though it is easy to see if the expression has a solution using software) We present the excitation spectrum for a gapless phase where  $J_x = J_y = J_z = 10$ . But, due to the limits of numerical computation, we see that the two minima don't actually touch: Now, we give the excitation spectrum for a borderline, gapped phase where  $J_x = J_y = 6$  and  $J_z = 12.5$ , in this case too, the minima are almost as distant as in the gapless phase:

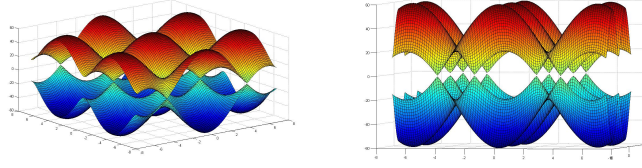


Figure 2.5: Gapless phase

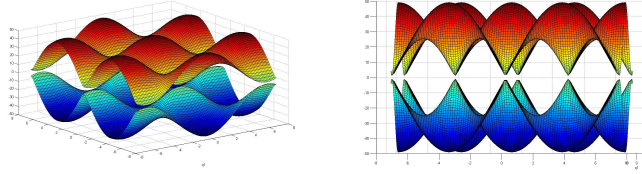


Figure 2.6: Borderline gapped phase

However, in a gapped phase far from the gapless phase, given by  $J_x = J_y = 6$  and  $J_z = 16$ , The minima are very well-separated:

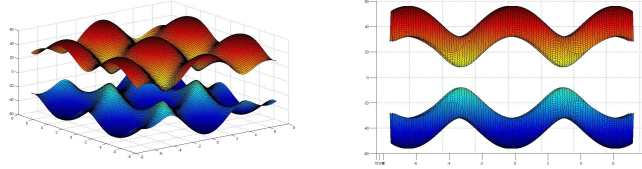


Figure 2.7: Gapped Phase

However, we can observe the changes in the minimum energy values as we move along the three different rays, OX,OY and OZ in the triangle(Figure 2.4). The three graphs are shown in Figure (2.8). A marked change in the minimum values can be observed in the final graphs which indicates a phase transition. And this occurs exactly where we would like it to be, at the point when the parameters invalidate the triangle inequality.

The Density of states(for 450 sites) for the vortex free case is given for different parameter values, as we go along the ray OZ in Figure(2.4) is given in Figure (2.9). As expected, the spectrum is gapped when the couplings don't satisfy triangle inequality and gapless otherwise.

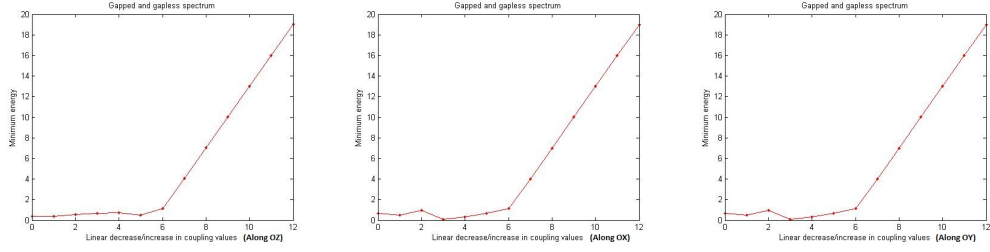


Figure 2.8: Phase transitions

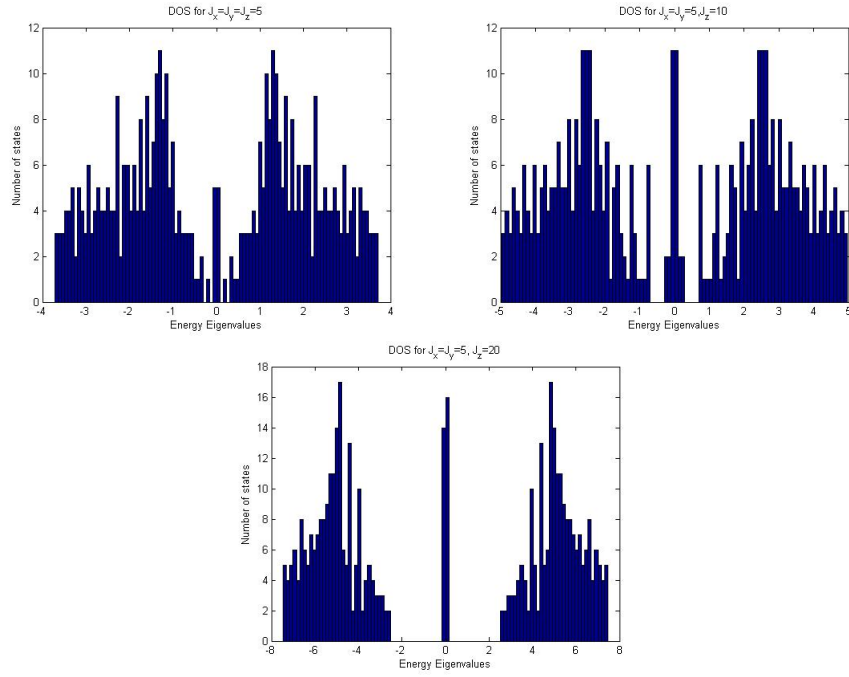


Figure 2.9: DOS for different coupling parameters

# Bibliography

- [1] Unpaired Majorana Fermions in Quantum Wires, A. Kitaev, 2001
- [2] Anyons in an exactly Solved Model And Beyond, A. Kitaev, 2008
- [3] Majorana Modes and Topological States in Realistic Driven-Dissipative Quantum Systems, Charles Edouard Bardyn
- [4] Kitaev model on the honeycomb and diamond lattices, Ludo Nieuwenhuizen
- [5] Introduction to Many Body Quantum Theory in Condensed Matter Physics, Henrik Bruus et.al
- [6] <http://physics.stackexchange.com/questions/261788/calculating-the-boundary-modes-in-kitaev-chain>
- [7] <http://physics.stackexchange.com/questions/199647/unpaired-majoranas-in-the-kitaev-chain>
- [8] Group theoretical and topological analysis of the quantum spin Hall effect in silicene, F. Geissler et.al.
- [9] Floquet Majorana Edge Mode and Non-Abelian Anyons in a Driven Kitaev Model, Masahiro Sato et.al.